

Enhancement of c-Myc degradation by BLM helicase leads to delayed tumor initiation

Suruchika Chandra, Raina Priyadarshini, Vinoth Madhavan, Shweta Tikoo, Mansoor Hussain, Richa Mudgal, Priyanka Modi, Vivek Srivastava and Sagar Sengupta*

National Institute of Immunology, Aruna Asaf Ali Marg, New Delhi 110067, India

*Author for correspondence (sagar@nii.res.in)

Accepted 16 May 2013

Journal of Cell Science 126, 3782–3795

© 2013. Published by The Company of Biologists Ltd

doi: 10.1242/jcs.124719

Summary

The spectrum of tumors that arise owing to the overexpression of c-Myc and loss of BLM is very similar. Hence, it was hypothesized that the presence of BLM negatively regulates c-Myc functions. By using multiple isogenic cell lines, we observed that the decrease of endogenous c-Myc levels that occurs in the presence of BLM is reversed when the cells are treated with proteasome inhibitors, indicating that BLM enhances c-Myc turnover. Whereas the N-terminal region of BLM interacts with c-Myc, the rest of the helicase interacts with the c-Myc E3 ligase Fbw7. The two BLM domains act as ‘clamp and/or adaptor’, enhancing the binding of c-Myc to Fbw7. BLM promotes Fbw7-dependent K48-linked c-Myc ubiquitylation and its subsequent degradation in a helicase-independent manner. A subset of BLM-regulated genes that are also targets of c-Myc were determined and validated at both RNA and protein levels. To obtain an *in vivo* validation of the effect of BLM on c-Myc-mediated tumor initiation, isogenic cells from colon cancer cells that either do or do not express BLM had been manipulated to block c-Myc expression in a controlled manner. By using these cell lines, the metastatic potential and rate of initiation of tumors in nude mice were determined. The presence of BLM decreases c-Myc-mediated invasiveness and delays tumor initiation in a mouse xenograft model. Consequently, in tumors that express BLM but not c-Myc, we observed a decreased ratio of proliferation to apoptosis together with a suppressed expression of the angiogenesis marker CD31. Hence, partly owing to its regulation of c-Myc stability, BLM acts as a ‘caretaker tumor suppressor’.

Key words: Bloom helicase, BLM, c-Myc, Fbw7, Colon carcinoma, E3 ligase

Introduction

Bloom syndrome (BS) is caused by mutation in the RecQ helicase family member, the helicase Bloom syndrome protein (BLM). The disorder is characterized by a predisposition to a wide spectrum of cancers (German, 1997). BS patients exhibit defects in DNA replication and homologous recombination events, manifested by an increased frequency of sister chromatid exchanges (SCEs) (Chaganti et al., 1974). BLM regulates homologous recombination by a number of mechanisms, such as disruption of RAD51 nucleofilaments (Bugreev et al., 2007; Tripathi et al., 2007), prevention of chromosome breakage (Russell et al., 2011), recruitment of p53 to carry out its own functions during homologous recombination (Sengupta et al., 2003) and enhancement of the interactions between 53BP1 and RAD51 (Tripathi et al., 2008; Tripathi et al., 2007). BLM is involved in the recognition of the DNA damage by a K63-linked ubiquitin-dependent mechanism (Tikoo et al., 2013), transmission of the damage signal to the repair proteins and in repair of the DNA damage during the effector phase (Tikoo and Sengupta, 2010). Hence, it can be argued that the proposed ‘caretaker tumor suppressor’ function of BLM (Hickson, 2003) is a culmination of the multiple roles of the helicase.

The proto-oncogene *MYC* encodes a DNA-binding factor (c-Myc) that can both activate and repress transcription (Dang et al., 2006). At the post-translational level c-Myc expression is controlled through sequential and reversible phosphorylation at two highly conserved residues, threonine 58 (Thr58) and serine 62

(Ser62) (Dai et al., 2006; Hann, 2006). This doubly phosphorylated c-Myc binds to its primary E3 ligase complex, which consists of SKP1, CUL1 and F-box proteins (hereafter referred to as SCF^{Fbw7}) both *in vitro* and *in vivo* (Welcker et al., 2004a; Welcker et al., 2004b; Yada et al., 2004). Alternatively, dephosphorylated Ser62 and phosphorylated Thr58 in c-Myc can also serve as a dock to recruit the SCF^{Fbw7} complex, leading to c-Myc ubiquitylation and proteasomal degradation (Yeh et al., 2004). Transcription of human *FBXW7* (hereafter referred to as FBW7) can yield three different transcripts (FBW7 α , FBW7 β and FBW7 γ) that are produced by alternative splicing (Welcker and Clurman, 2008). The level of c-Myc is regulated by the nucleolar Fbw7 γ and nucleoplasmic Fbw7 α (Grim et al., 2008; Welcker et al., 2004a).

It is known that cells from BS patients have high levels of c-Myc protein (Sullivan et al., 1989; West et al., 1995). The spectrum of tumors associated with the overexpression of c-Myc (Nesbit et al., 1999) and the loss of BLM (as in BS patients and BLM-knockout mice) (Hickson, 2003) are also strikingly similar. Hence, we wanted to test the hypothesis that BLM negatively regulates c-Myc functions. Our results indicate that BLM, indeed, promotes the Fbw7-dependent ubiquitylation and degradation of c-Myc, subsequently causing a delay in c-Myc-dependent initiation of tumors.

Results

BLM regulates c-Myc stability via Fbw7

To determine whether BLM affects endogenous levels of SCF^{Fbw7} substrates, we compared the levels of five such

substrates (c-Myc, cyclin E, c-Jun, B-MyB and KLF5) in three isogenic pairs of cell lines that either do or do not express BLM. Endogenous levels of c-Myc, cyclin E and c-Jun were higher in BS, GM08505+GFP and HCT116 BLM^{-/-} cells when compared with A-15 cells (Fig. 1A), GM08505 + GFP-BLM (Fig. 1B) and wild-type HCT116 cells (Fig. 1C), respectively. However, we did not detect any change in the levels of B-MyB and KLF5 in cells that express and do not express BLM (our unpublished data), indicating that the effect of BLM occurs only on a subset of SCF^{Fbw7} substrates. The increase in the levels of SCF^{Fbw7} substrates was also not observed in cells obtained from patients suffering from Werner syndrome or Rothmund-Thomson Syndrome, disorders that are caused by gene mutations of two other members of the RecQ helicase family, *WRN* and *RECQL4*, respectively (supplementary material Fig. S1A,B).

To determine whether the role of BLM on the levels of SCF^{Fbw7} substrates was at the transcriptional level, northern hybridization, reverse transcriptase (RT)-PCR and real-time PCR analysis were carried out (supplementary material Fig. S1C-E).

All the above techniques indicated that the RNA levels of *Myc* were not substantially altered in presence or absence of BLM. Furthermore, similar levels of c-Myc, cyclin E and c-Jun in BS and A-15 cells were observed after treatment with proteasomal inhibitors, MG132 (Fig. 1D,E) or LLnL (supplementary material Fig. S1F). The rate of turnover of endogenous c-Myc was also found to be higher in cells that express BLM, which was determined by treating the cells with protein synthesis inhibitor cycloheximide (Fig. 1F) or by pulse labeling the cells (supplementary material Fig. S1G). The half-life of c-Myc in REF52 cells grown in presence of serum is ~90 minutes (Sears et al., 1999). We found that the half-life of c-Myc increased from 96 minutes in A-15 cells to 310 minutes in BS cells (Fig. 1F, right).

To determine whether the BLM and the three SCF^{Fbw7} substrates c-Myc, cyclin E and c-Jun physically interact, GST pull-down assays were carried out with wild-type BLM (1-1417) (supplementary material Fig. S2A,B), using cyclin E, c-Jun or c-Myc. *In vitro* interaction assays indicated that BLM interacted

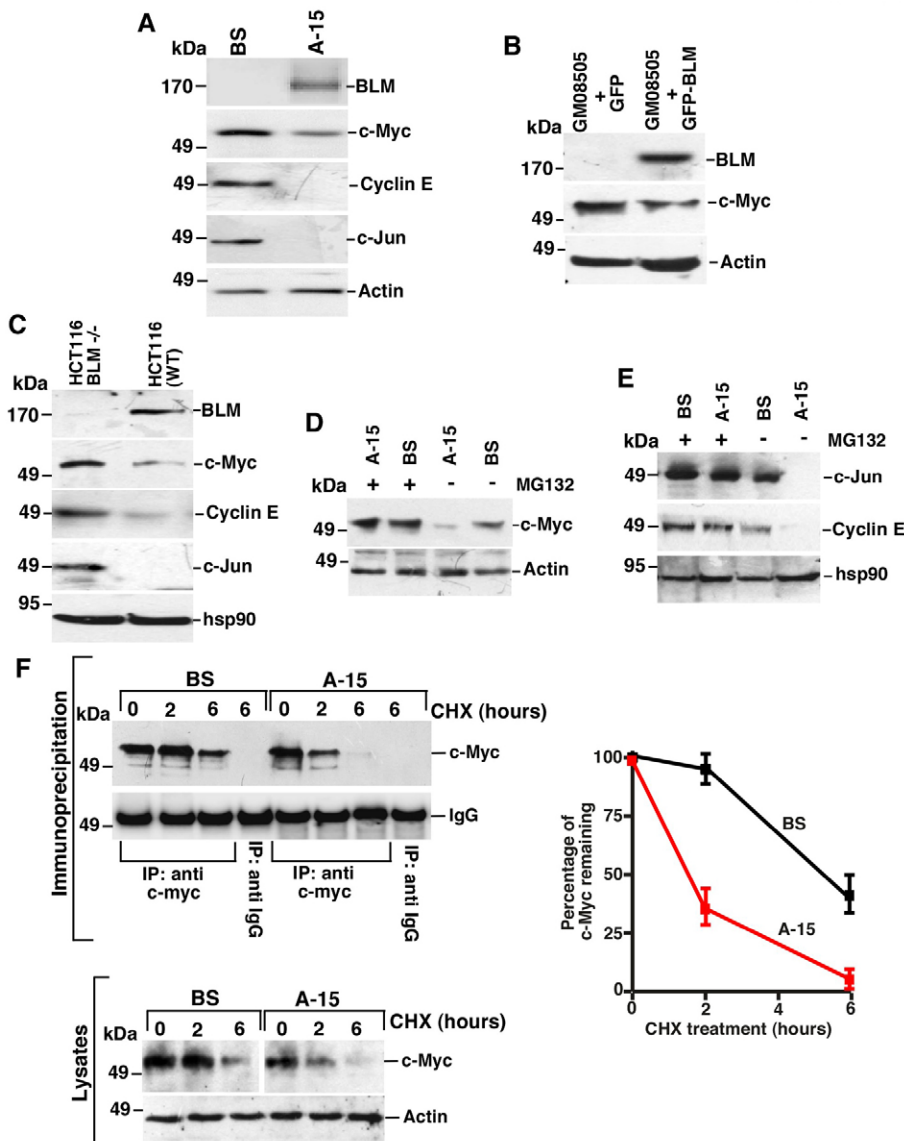


Fig. 1. BLM decreases the stability of SCF^{Fbw7} substrates. (A-C) Presence of BLM decreases the level of c-Myc, c-Jun and cyclin E. The levels of BLM, c-Myc, cyclin E, c-Jun were determined in isogenic cell lines (A) BS, A-15; (B) GM08505 + GFP, GM08505 + GFP-BLM; (C) HCT116 BLM^{-/-}, HCT116. Whole-cell lysates were prepared and blots probed as indicated with antibodies against BLM (ab476), c-Myc (13-2500), cyclin E, c-Jun, hsp90 and actin. (D-E) Decrease in the levels of c-Myc, c-Jun and cyclin E is reversed in the presence of the proteasomal inhibitor MG132. Nuclear extracts prepared from A-15 and BS cells were either left untreated or treated with MG132. The blots are probed with antibodies against c-Myc (13-2500), cyclin E, c-Jun and hsp90. (F) Half-life of c-Myc is enhanced in the absence of BLM. Whole-cell extracts were prepared from BS and A-15 cells that were either not treated with cycloheximide (CHX) (0 hours) or treated with CHX for the indicated periods (bottom, left). The nuclear extracts were immunoprecipitated with antibody against c-Myc (13-2500), probed with antibody against c-Myc (#9402). IgG (heavy chain) acts as a control for the amount of the antibody used during immunoprecipitation (top, left). Quantification of c-Myc levels at different intervals after cycloheximide exposure (right). The graph shows the percentage of c-Myc levels (mean \pm s.d.) of three experiments.

with all three tested SCF^{Fbw7} substrates (Fig. 2A,B). Specifically the N-terminal region of BLM interacted with the C-terminal region of c-Jun, which contains the DNA-binding domain and leucine zipper module (Fig. 2A, middle and bottom blot, and supplementary material Fig. S2C). The N-terminal region of BLM also interacted with c-Myc (Fig. 2B, right). The c-Myc–BLM interaction was not diminished when c-Myc was mutated at

Thr58 and Ser62 (Fig. 2C). On the basis of the interaction studies with the C-terminal fragments, it was deduced that amino acids 300–410 of c-Myc – which encompass the basic region and the helix loop helix (HLH) – minimally interacts with BLM (Fig. 2D,E; supplementary material Fig. S2D,E). However, due to the inherent flaws that can happen due to fragment-based analysis, two new c-Myc fragments were generated, namely c-Myc

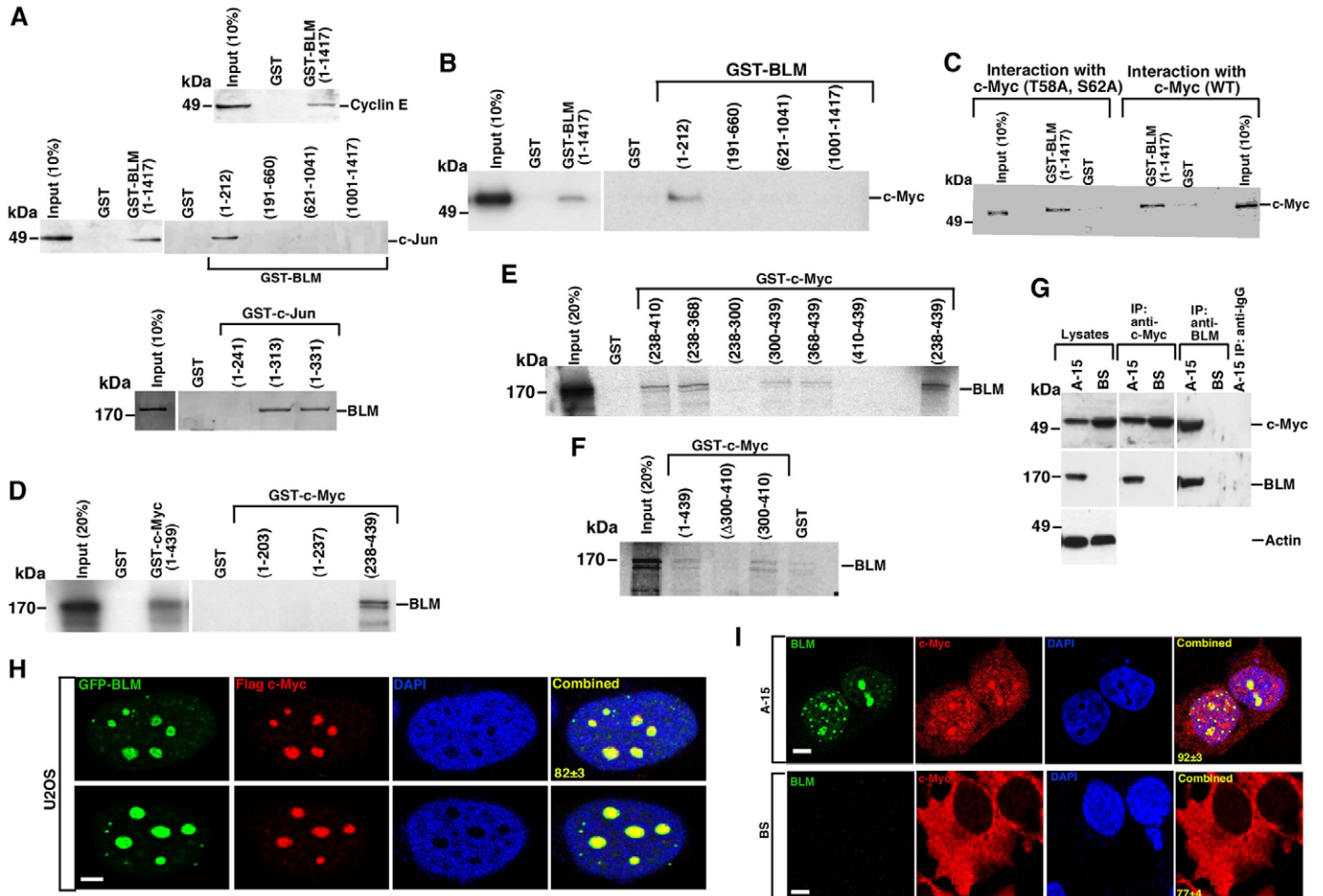


Fig. 2. BLM interacts with c-Myc and colocalizes predominantly in the nucleolus. (A) BLM interacts with cyclin E and c-Jun. (Top) *In vitro* translated S³⁵-methionine radiolabeled cyclin E was incubated with equalized amounts of Glutathione S-Sepharose-bound GST-tagged BLM (1–1417) or GST. (Middle) *In vitro* translated S³⁵-methionine radiolabeled c-Jun was incubated with equalized amounts of Glutathione S-Sepharose-bound GST-tagged BLM (1–1417), BLM (1–212), BLM (191–660), BLM (621–1041) and BLM (1001–1417). (Bottom) *In vitro* translated S³⁵-methionine radiolabeled BLM was incubated with equalized amounts of Glutathione S-Sepharose-bound GST-tagged c-Jun (1–214), c-Jun (1–313) and c-Jun (1–331). All the bound proteins were detected by autoradiography. (B–C) The N-terminal region of BLM interacts with c-Myc. (B) *In vitro* translated S³⁵-methionine radiolabeled c-Myc (1–454) was incubated with equalized amounts of Glutathione S-Sepharose bound GST-tagged BLM (1–1417), BLM (1–212), BLM (191–660), BLM (621–1041), BLM (1001–1417) or GST alone. Bound c-Myc is detected by autoradiography. (C) Same as B, except that GST-BLM (1–1417) or GST was incubated with S³⁵-methionine radiolabeled c-Myc (WT) or c-Myc (T58A, S62A). (D) C-terminal region of c-Myc interacts with BLM. Same as B, except S³⁵-methionine radiolabeled BLM was used. Incubations were with Glutathione S-Sepharose-bound GST-tagged c-Myc (1–439), c-Myc (1–203), c-Myc (1–237), c-Myc (238–439). (E) The region encompassing the NLS, basic region and helix-loop-helix (HLH) region interact with BLM. Same as B, except that S³⁵-methionine radiolabeled BLM was incubated with GST-c-Myc (238–410), c-Myc (238–368), c-Myc (238–300), c-Myc (300–439), c-Myc (368–439), c-Myc (410–439) and c-Myc (238–439). (F) The minimal interacting region (amino acids 300–410) in c-Myc interacts with BLM. Same as E, except that GST-c-Myc (1–439), GST-c-Myc (Δ300–410) and GST-c-Myc (300–439) were used. (G) Endogenous BLM and c-Myc interact. Nuclear extracts from BS and A-15 cells were immunoprecipitated with antibody against c-Myc (13-2500) or BLM (ab476). The immunoprecipitates were probed with the reciprocal antibodies [c-Myc (#9402), BLM (ab476)]. Anti-actin antibody was used as the loading control. (H–I) c-Myc and BLM colocalize. (H) Localization of transfected FLAG-tagged c-Myc and EGFP-BLM was determined by immunofluorescence. EGFP fluorescence and staining experiments were carried out using antibody against the FLAG tag. The nucleus was stained using DAPI. The number in the panels labeled 'combined' (merged images) panels represents the percentage of colocalization of GFP-BLM and FLAG-c-Myc in the transfected cells. Two representative cells are shown. Scale bars: 5 μm. (I) Same as H, except that endogenous c-Myc (stained by N-262) and BLM (stained by A300-120A) were visualized in BS and A-15 cells. The number in the panels labeled 'combined' (merged images) show the percentage of cells with BLM–c-Myc colocalization. Scale bars: 5 μm.

(300–410) and Myc (Δ 300–410) (supplementary material Fig. S2D,E). We hoped that Myc (Δ 300–410), which was generated on the entire c-Myc, would not interact with BLM and, indeed, found that Myc (300–410) but not Myc (Δ 300–410), interacts with BLM (Fig. 2F). Reciprocal immunoprecipitations by using either antibodies against c-Myc or BLM (Fig. 2G) indicated that, *in vivo*, the two endogenous proteins constitutively interact. Both BLM and c-Myc have been separately reported to localize to the nucleoli (Arabi et al., 2005; Yankiwski et al., 2000), the subnuclear compartment implicated for c-Myc degradation (Arabi et al., 2005; Welcker et al., 2004a). Immunofluorescence staining with ice-cold methanol:acetone fixation indicated that overexpressed Myc and BLM were present in both nucleoplasm and nucleolus (identified by DAPI exclusion). BLM and c-Myc colocalized extensively in the nucleolus and, to a limited extent, in the nucleoplasm (Fig. 2H). Endogenous c-Myc and BLM in A-15 cells also colocalized in both nucleolus and nucleoplasm (Fig. 2I). However, Myc-BLM colocalization was not observed in the PML nuclear bodies, where BLM was also found. Compared with A-15 cells, the endogenous c-Myc in BS cells was substantially more cytoplasmic (Fig. 2I). This might indicate a role of BLM in the transport of c-Myc from the cytoplasm to the nucleus.

The ubiquitylation and subsequent degradation of c-Myc in cells can occur either by phosphorylation-dependent or independent mechanisms that are mediated by two different E3 ligases of c-Myc, namely Fbw7 and Skp2 (Kim et al., 2003; Yada et al., 2004). Additionally, a conserved phosphodegron in c-Myc consisting of a central phosphothreonine residue followed by a cysteine and an additional priming phosphodegron by GSK3 β in the +4 position is required (Welcker and Clurman, 2008). So the effect of BLM on c-Myc ubiquitylation and degradation could be

a reflection of the activity of GSK3 β or the levels of the two E3 ligases that are known to be involved in c-Myc degradation. Using two independent assay techniques, we found that the extent of phosphorylation of GSK3 β serine 9 (a marker for the intracellular active GSK3 β) is similar in cells expressing and not expressing BLM (Fig. 3A). This indicated that differential GSK3 β signaling did not depend on the absence or presence of the helicase. By using a validated antibody against Fbw7 (Fig. 3B), the endogenous levels of Fbw7 and Skp2 were found to be similar in A-15 and BS cells (Fig. 3C). Interestingly, BLM interacted specifically with Fbw7 but not Skp2 (Fig. 3D).

BLM enhanced the binding of Fbw7 with c-Myc

Since BLM affected c-Myc stability (Fig. 1) and also interacted with c-Myc (Fig. 2), we hypothesized that BLM directly modulates the interaction of c-Myc with its E3 ligase Fbw7. *In vitro* interaction assays carried out with all the three isoforms of Fbw7 (supplementary material Fig. S3A) indicated that the E3 ligase interacts with GST-tagged BLM (1–1417) but not to GST alone (Fig. 4A). Ability of BLM to interact with Fbw7 (Δ N) (Fig. 4A) indicates that BLM–Fbw7 interaction occurs through the common C-terminal dimerization, F box and WD40 domains of the Fbw7 isoforms. Since BLM is a nuclear protein, we were interested in the interaction between BLM–Fbw7 α and BLM–Fbw7 γ . Hence, to determine the subnuclear location where BLM could interact with Fbw7, we carried out immunofluorescence staining following the overexpression of the tagged version of the two proteins (because endogenous Fbw7 could not be detected by any available antibody against Fbw7 in immunofluorescence experiments). As known in literature (Yankiwski et al., 2000) BLM was observed in both nucleus and nucleoplasm. In these

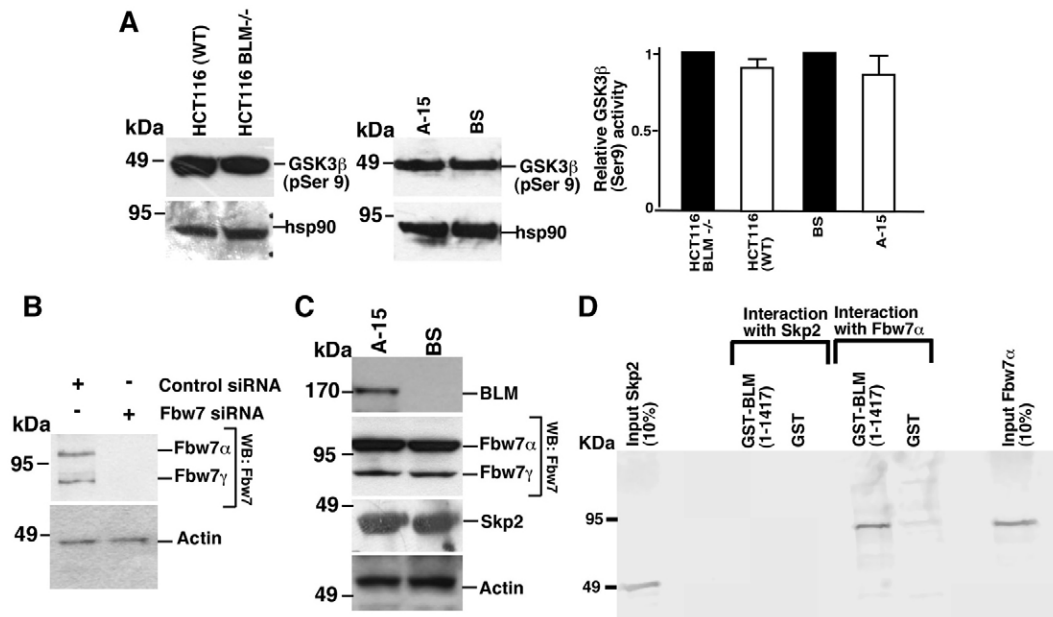


Fig. 3. BLM specifically utilizes Fbw7 to regulate the levels of c-Myc. (A) GSK3 β is equally active in absence or presence of BLM. Whole-cell extracts from HCT116 (WT)/HCT116 BLM^{-/-} or A-15 and BS cells were used to determine the activity of GSK3 β either by western analysis with antibody against GSK3 β (pSer9) (left) or by using an activity assay kit (right). (B) Levels of Fbw7 are decreased following transfection of Fbw7 siRNA. Fbw7 siRNA or control siRNA were transfected into A-15 cells. Nuclear extracts were probed with antibodies against Fbw7 and actin. (C) Levels of Fbw7 and Skp2 were unchanged in the absence of BLM. Whole-cell extracts from asynchronously growing BS and A-15 cells were probed with antibodies against BLM (ab476), Fbw7, Skp2 and actin. (D) BLM interacts with Fbw7 α and not Skp2. *In vitro* translated S³⁵-methionine radiolabeled Fbw7 α or Skp2 has been incubated with equal amounts of Glutathione S-Sepharose-bound GST-tagged BLM (1–1417) or GST. Bound Fbw7 α was detected by digital autoradiography with a phosphorimager plate.

two subnuclear compartments BLM colocalized with either Fbw7 α in the nucleoplasm or with Fbw7 γ in the nucleolus (Fig. 4B).

The above results led to the hypothesis that BLM simultaneously binds to both c-Myc and Fbw7. We found that, except the N-terminal (1–212) amino acids, the rest of BLM interacts with both Fbw7 α and Fbw7 γ (Fig. 4C). The interaction of BLM with Fbw7 was also observed using a BLM recombinant protein that lacked the first 212 amino acids (our unpublished

observations), thereby verifying the authenticity of the interaction. Since two distinct regions of BLM interacted with c-Myc and Fbw7, we hypothesized that maybe BLM acts as a ‘clamp/adaptor’ protein, thereby enhancing c-Myc interaction with Fbw7. To test this hypothesis, assays were carried for which we used bacterially expressed differently tagged recombinant proteins (Fig. 4D) or a combination of recombinant and *in vitro* translated proteins (supplementary material Fig. S3B). In both the assays, the addition of wild-type BLM (1–1417) enhanced the

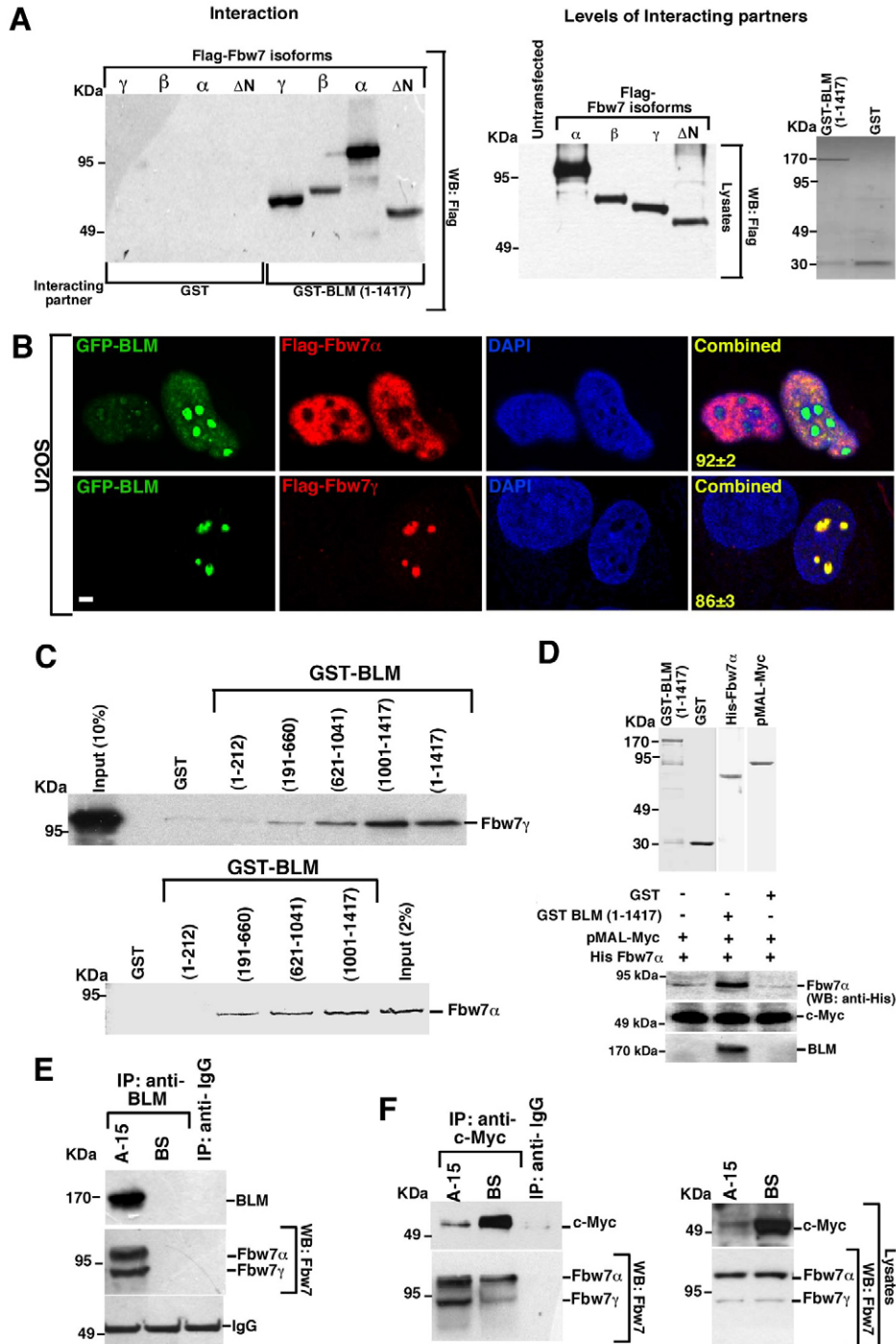


Fig. 4. See next page for legend.

interaction between c-Myc and Fbw7 α (Fig. 4D; supplementary material Fig. S3B top panel). The use of bacterially produced purified proteins (Fig. 4D) also indicated that the interactions observed when using *in vitro* translated proteins (Fig. 2; supplementary material Fig. S3B) were authentic and not due to the presence of additional cellular proteins that may have been present in the rabbit reticulocyte system. *In vivo*, endogenous BLM interacted with both Fbw7 α and Fbw7 γ (Fig. 4E). Furthermore, we observed increased levels of endogenous Fbw7 isoforms that were able to form complexes with endogenous c-Myc in A-15 cells; this was despite the presence of more endogenous c-Myc in BS cells (Fig. 4F). Altogether these results indicate that BLM enhanced the binding of c-Myc to Fbw7.

Phosphorylation of c-Myc at Thr58/Ser62 is an important parameter for its ubiquitylation-dependent degradation (Welcker et al., 2004a; Welcker et al., 2004b; Yada et al., 2004) by Fbw7. Hence, we wanted to determine whether the level of c-Myc phosphorylated at Thr58 and Ser62 was altered in absence of BLM. Using a validated antibody against phosphorylated c-Myc (Thr58/Ser62) (supplementary material Fig. S3C), more Thr58/Ser62 biphosphorylated c-Myc forms were observed in A-15 cells (supplementary material Fig. S3D), even though the levels of total c-Myc was found to be higher in BS cells. However, the presence of either GSK3 β inhibitor or λ phosphatase did not abolish the effect of BLM on the interaction between c-Myc and

Fbw7 (supplementary material Fig. S3B, middle panel). Moreover, wild-type BLM enhanced the physical interaction of Fbw7 with wild-type and mutant (T58A, S62A) c-Myc to equal extent (supplementary material Fig. S3E). Together, these results (supplementary material Fig. S3B, middle panel and S3E) indicate that BLM-mediated enhancement of Fbw7-Myc interaction does not depend on the phosphorylation of c-Myc residues Ser58 and Thr62.

BLM enhanced Fbw7-mediated K48-linked c-Myc ubiquitylation

On the basis of the above results, we wanted to test whether BLM has a stimulatory effect on Fbw7-dependent c-Myc ubiquitylation. First, we verified that the Fbw7 that we used can act as an E3 ligase for c-Myc over a variety of concentrations (supplementary material Fig. S4A). The authenticity of the c-Myc ubiquitylation by Fbw7 was also verified by using a F-box deletion (Fbw7 $\gamma\Delta F$) mutant. As expected, the Fbw7 $\gamma\Delta F$ mutant showed loss of c-Myc ubiquitylation (supplementary material Fig. S4B).

Next, we wanted to determine whether full-length recombinant BLM has any effect on Fbw7-dependent c-Myc ubiquitylation. For these assays we used Fbw7, which led to a minimal level of c-Myc ubiquitylation, consequently allowing us to better visualize the effect of BLM. The amount of *in vitro* translated c-Myc used for the ubiquitylation reactions was the same in all experiments (Fig. 5A, middle panel). BLM (1–1417) enhanced Fbw7-mediated c-Myc ubiquitylation *in vitro*, as detected by using antibody against c-Myc. The extent of enhancement was the same for Fbw7 γ and Fbw7 α (Fig. 5A, top panel). The blot was subsequently probed with antibody against FK2, which recognized both mono- and poly-ubiquitylated conjugates. BLM enhanced both mono- and poly-ubiquitylation of c-Myc (Fig. 5A, middle panel). A helicase-dead BLM (K695A) mutant also stimulated ubiquitylation to the same extent as wild-type BLM (Fig. 5B), indicating that the stimulatory function of BLM on c-Myc ubiquitylation was not dependent on its DNA unwinding activity.

Next we wanted to determine the effect of BLM on Fbw7-mediated c-Myc ubiquitylation in context of its known requirement for phosphorylation at Thr58 and Ser62 residues. Interestingly, the effect of BLM on c-Myc ubiquitylation was less for the c-Myc (T58A, S62A) mutant when compared with wild-type c-Myc (supplementary material Fig. S4C). Moreover, BLM could not stimulate Fbw7 γ -dependent c-Myc ubiquitylation in presence of either GSK3 β inhibitor (Fig. 5C) or λ phosphatase (supplementary material Fig. S4D). Together, these results provide evidence that the GSK3 β -dependent phosphorylation of c-Myc at Ser58 and Thr62 residues is a prerequisite for BLM in order to enhance c-Myc ubiquitylation.

To show that BLM, indeed, regulates c-Myc ubiquitylation *in vivo*, reciprocal immunoprecipitations with either anti-K48-linked ubiquitin (Fig. 5D) or c-Myc (Fig. 5E) were carried out. Although more endogenous c-Myc was present in the BS cells, K48-linked ubiquitylated forms of c-Myc were enhanced in A-15 cells (Fig. 5D,E). Hence, depletion of Fbw7 in A-15 cells through corresponding small interfering RNA (siRNA) (validated by the stabilization of c-Myc) (Fig. 5F, right) led to a huge decrease of c-Myc ubiquitylation in A-15 cells (Fig. 5F, left), providing evidence that the presence of BLM enhanced Fbw7-mediated c-Myc degradation *in vivo*.

Fig. 4. BLM enhances the interaction of c-Myc with Fbw7. (A) BLM interacts with Fbw7 isoforms. GST-tagged recombinant BLM or GST alone (extreme right) is incubated with whole-cell extracts of 293T-cells expressing FLAG-tagged Fbw7 isoforms or ΔN Fbw7 α (middle). Post interaction, bound Fbw7 isoforms are detected using antibody against the FLAG tag (left). (B) Colocalization of BLM with Fbw7 isoforms. GFP-BLM and Fbw7 isoforms were transfected into U2OS cells. The overexpressed proteins were detected through GFP fluorescence (for BLM) and by staining with antibody against the FLAG tag (for Fbw7 isoforms). Nuclei were stained using DAPI. The number in the panels labeled 'combined' (merged images) represent the percentage of cells showing colocalization of GFP-BLM and Flag-Fbw7 isoforms. Scale bars: 5 μ m. (C) The C-terminal region of BLM interacts with Fbw7 α and Fbw7 γ . *In vitro* translated, S³⁵-methionine radiolabeled Fbw7 α (top) or Fbw7 γ (bottom) were incubated with equalized amounts of Glutathione S-Sepharose-bound wild type BLM (1–1417), BLM (1–212), BLM (191–660), BLM (621–1041) and BLM (1001–1417). GST protein was used as negative control. Bound Fbw7 α or Fbw7 γ was detected by autoradiography. (D) BLM enhances the interaction of c-Myc with Fbw7 α . (Top) Recombinant GST-tagged BLM (1–1417), His-tagged Fbw7 α and pMAL-c-Myc were all generated in *E. coli* and checked for purity by polyacrylamide gel electrophoresis stained with Coomassie Blue. (Bottom) Incubation of amylose-resin-bound c-Myc (0.01 nM) with soluble His-tagged Fbw7 α (0.01 nM) in absence or in presence of soluble BLM (1–1417) (0.01 nM) or GST (0.01 nM). Fbw7 α bound to c-Myc was detected by western blot analysis with antibody against the polyHistidine tag. The levels of c-Myc and BLM have been verified using antibodies against BLM (A300-110A) and c-Myc (13-2500). (E) Endogenous BLM interacts with Fbw7 isoforms. Immunoprecipitation of BLM (ab476) antibody with nuclear extracts from BS and A-15 cells. The immunoprecipitates were probed with antibodies against BLM (ab476) and Fbw7. IgG (heavy chain) was used as a control for the amount of antibody. (F) Endogenous BLM enhances c-Myc-Fbw7 interaction *in vivo*. Immunoprecipitations with antibody against c-Myc (13-2500) were carried out with nuclear extracts from BS and A-15 cells. The immunoprecipitates have been probed with anti-c-Myc (#9402) and anti-Fbw7 antibodies (left). The levels of c-Myc and Fbw7 in the lysates from A-15 and BS cells were determined by using the same antibodies (right).

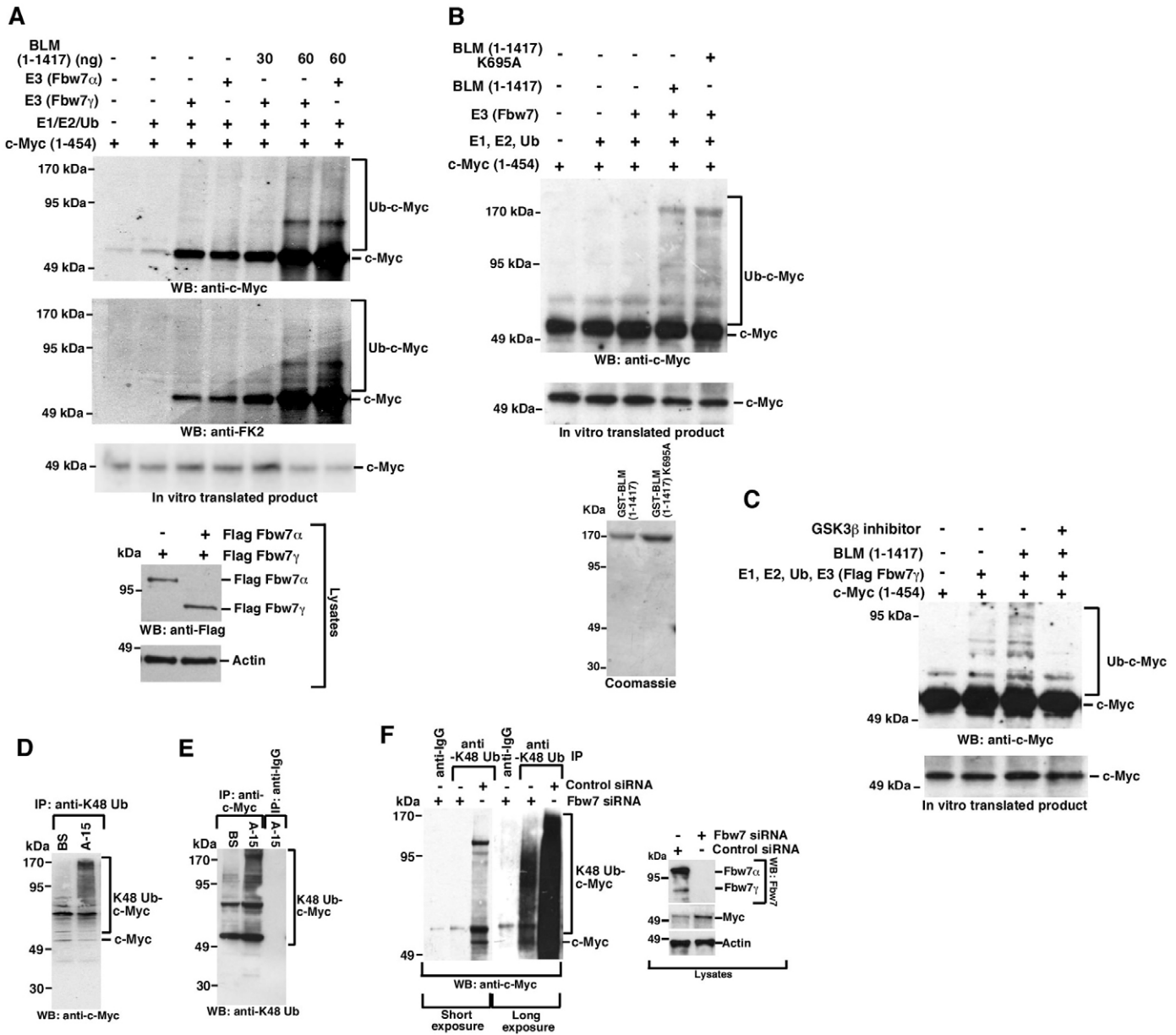


Fig. 5. BLM enhances Fbw7-mediated c-Myc ubiquitylation. (A) Full-length BLM enhances Fbw7 α - and Fbw7 γ -mediated c-Myc ubiquitylation *in vitro*. Ubiquitylation reactions of c-Myc (1-454) were carried out with either Fbw7 α or Fbw7 γ as the E3 ligase, in absence or presence of wild-type BLM (30 ng for Fbw7 α and 30 ng and 60 ng for Fbw7 γ). Ubiquitylated forms of c-Myc were detected by probing with anti-c-Myc (#9402) antibody (top) and, subsequently, with anti-FK2 antibody (middle). Equal amounts of Fbw7 α and Fbw7 γ were used as determined by western blot analysis with anti-Flag antibody (bottom). (B) BLM enhances Fbw7 γ -mediated c-Myc ubiquitylation in a helicase-independent manner. Ubiquitylation reactions have been carried out as in A. Equal amounts (30 ng) of BLM (1-1417) or BLM (1-1417) K695A were used. Ubiquitylated c-Myc forms were detected by anti-c-Myc (#9402) antibody (top). The amount of *in vitro* translated c-Myc utilized is represented (middle). The purity of the BLM proteins was assessed by polyacrylamide gel electrophoresis stained with Coomassie Blue. (bottom). (C) Presence of GSK3 β inhibitor prevents BLM-dependent enhancement of c-Myc ubiquitylation. Ubiquitylation reactions were carried out as in A, except that the reactions were carried out in absence or presence of the preincubation with GSK3 β inhibitor. Ubiquitylated c-Myc forms were detected by anti-c-Myc (#9402) antibody (top). The amount of *in vitro* translated c-Myc utilized is represented (bottom). (D-E) BLM enhances K48-linked c-Myc ubiquitylation *in vivo*. Nuclear extracts from BS and A-15 cells have been immunoprecipitated with either (D) anti-K48-linked polyubiquitin (Apu2.07) or (E) c-Myc (13-2500) antibody. The immunoprecipitates have been probed with either anti-c-Myc (#9402) or anti-K48-linked polyubiquitin (Apu2.07) antibody. The samples were boiled in SDS-PAGE loading buffer before the analysis. (F) Enhancement of K48-linked c-Myc ubiquitylation *in vivo* by BLM was dependent on Fbw7. Same as D-E, except that the A-15 cells were transfected with either control siRNA or Fbw7 siRNA. The nuclear extracts were immunoprecipitated with anti-K48 linked polyubiquitin (Apu2.07) antibody and probed with c-Myc antibody. Two separate exposures of the c-Myc blot are shown (left). The levels of Fbw7 isoforms and c-Myc [detected with anti-Fbw7 and anti-c-Myc (#94102) antibodies] after Fbw7 siRNA or Control siRNA transfection are also depicted (right).

BLM regulates the expression of c-Myc target genes

We hypothesized that, by enhancing Fbw7-mediated c-Myc ubiquitylation and subsequent degradation, BLM can also affect the mRNA expression profiles of the c-Myc target genes. At first, to determine the genes whose transcript expression profile depend on BLM, we carried out microarray hybridization on mRNA extracted from BS/A-15 cells. Altogether, 2332 genes were differentially expressed due to the lack of BLM in BS cells; a detailed analysis of which will be reported later. Next, we wanted to determine the c-Myc target genes that are deregulated in A-15 cells. However, it was not possible to obtain complete depletion of endogenous c-Myc in A-15 cells and, thereby, we were unable to carry out a subsequent microarray in A-15 cells (with or without c-Myc). Hence, for the next stage the 2332 BLM-dependent genes were compared with the non-redundant 1672 genes listed in the c-Myc target database (www.myc-cancer-gene.org/) (Zeller et al., 2003), and whose expression was reported to be either activated or repressed by c-Myc. Comparison of the two gene lists indicated that 131 c-Myc

target genes were differentially expressed in BS and A-15 cells (supplementary material Table S1). These genes (7.8% of all c-Myc target genes and 5.6% of all the genes differentially regulated owing to the absence of BLM) qualified to be the c-Myc targets whose expression was regulated by BLM. Out of the 131 genes, 64 genes were upregulated while 67 were downregulated to a variable extent in the absence of BLM (Fig. 6A,B; supplementary material Table S1). Since only 131 out of 1672 c-Myc target genes were regulated by BLM, other factors possibly regulate the rest of the c-Myc target genes through parallel regulatory processes.

To validate the above analysis, mRNA expression pattern of c-Myc target genes differentially expressed in BS and A-15 cells were verified at the RNA level either by RT-PCR (Fig. 6C; supplementary material Table S2) or by real-time PCR (supplementary material Table S2). mRNA transcript patterns of the same set of genes were also checked in a second isogenic pair of cell lines (HCT116 BLM and HCT116 BLM^{-/-}) cells by RT-PCR (supplementary material Table S2). Gene expression

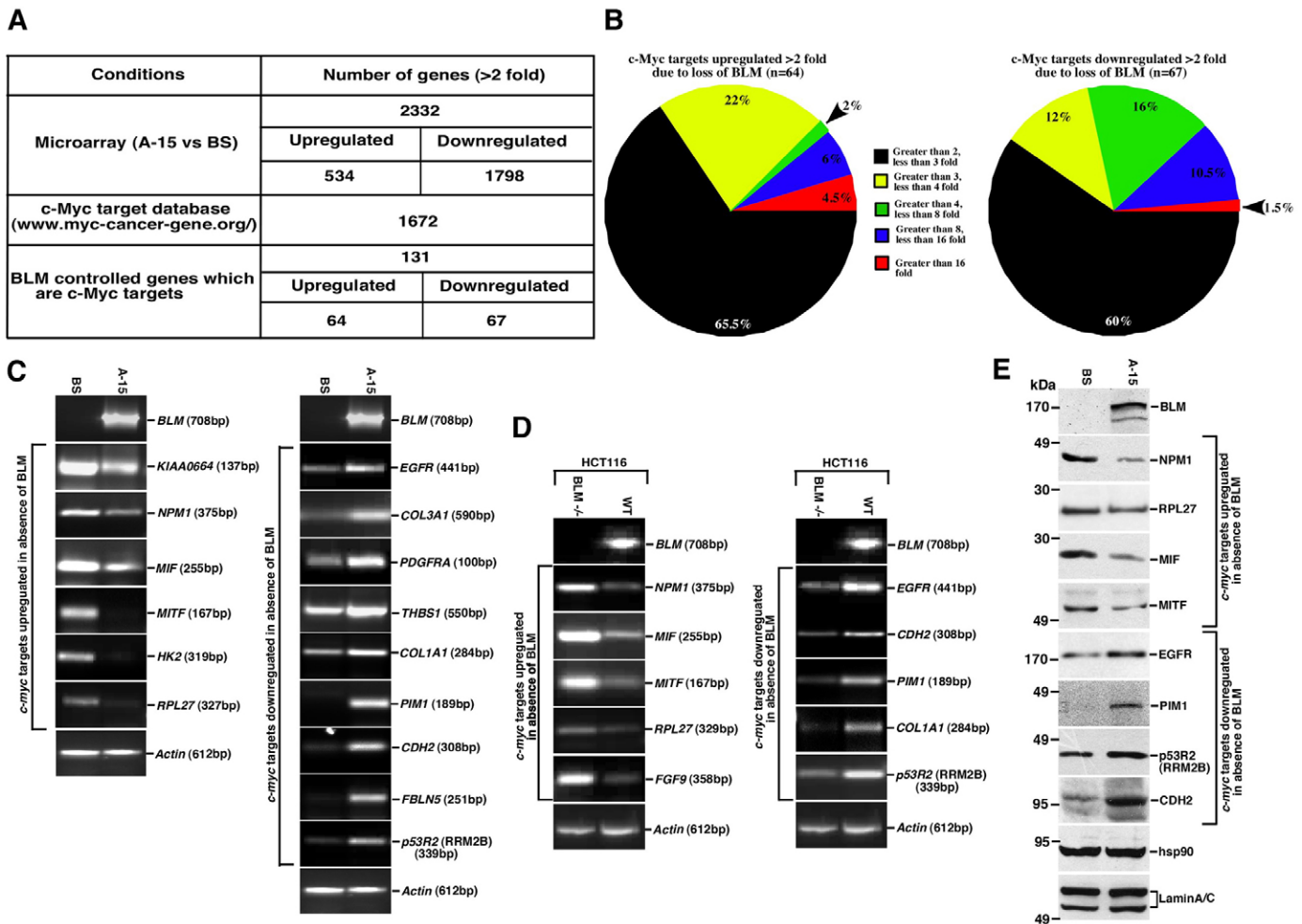


Fig. 6. BLM regulates the expression of c-Myc target genes. (A) Summary of c-Myc target genes whose expressions are regulated by BLM. (B) Diagram representing the percentage of distribution of c-Myc target genes whose transcription are either upregulated ($n=64$) (left) or downregulated ($n=67$) (right) in BS cells. (C-D) RNA expression of a subset of c-Myc target genes depends on BLM status. A subset of the 131 c-Myc target genes has been validated for BLM dependent transcript expression by RT-PCR using RNA isolated from (C) BS and A-15 cells and (D) HCT116 BLM^{-/-} and HCT116 cells. (E) Protein levels of a subset of c-Myc target genes depend on BLM. A subset of the 131 c-Myc target genes has been validated for BLM dependent protein expression by western analysis using the indicated antibodies on whole cell extracts obtained from BS and A-15 cells.

patterns of 34 out of the 67 downregulated genes and 32 out of the 64 upregulated genes (66 out of the 131 genes i.e. 50.3% of the total subset) were analysed cumulatively by using RT-PCR and real-time PCR. By these analyses, 28 out of the 34 c-Myc target genes (82.3%) whose expression was reported to be downregulated by the expression of BLM were verified. Similarly, in 25 out of the 32 target genes (78.1%) expression was found to be upregulated by the absence of BLM (supplementary material Table S2, yellow shaded genes). Hence, gene expression analysis through multiple procedures established that at least 53 out of the 131 c-Myc target genes (40.4%) were regulated by BLM. Since the analysis had been carried out for only 66 out of the original 131 genes, a further increase in the number of BLM-regulated c-Myc target genes is anticipated. Interestingly, expression patterns for 16 out of the analyzed 66 c-Myc target genes (ten genes which were downregulated and six genes which were upregulated, cumulatively 24.2% of the total genes analyzed) were reversed in absence of BLM (supplementary material Table S2, red shaded genes). Validation of protein expression of a subset of these genes was carried out in A-15 and BS cells (Fig. 6E; supplementary material Table S2), and at both RNA and protein level by transiently decreasing the expression of BLM in A-15 cells while expressing its cognate siRNA (supplementary material Fig. S4E,F). Hence, by enhancing c-Myc degradation, BLM also regulates the expression of a subset of c-Myc target genes.

BLM inhibits c-Myc driven tumor initiation in a mouse xenograft model

On the basis of the above results, it is possible that c-Myc functions on proliferative pathways were altered by the presence or absence of BLM. To test our hypothesis we generated a set of isogenic stable cell lines with the genotypes BLM⁺ c-Myc⁺, BLM⁺ c-Myc⁻, BLM⁻ c-Myc⁺ and BLM⁻ c-Myc⁻. We could not use the A-15 and BS cell lines for this purpose because these fibroblast derivatives do not have tumorigenic potential (our unpublished data). Hence, two new cell lines, HCT116 sh-Myc (Clone #9 and #7) and HCT116 BLM^{-/-} sh-Myc (Clone #5 and #13), were generated by stably coexpressing the Tet repressor (pcDNA6TR) and small hairpin RNA (shRNA) against c-Myc (pTER *c-myc*) (van de Wetering et al., 2003) in HCT116 and HCT116 BLM^{-/-} cells. These cells, which express tetracycline-regulated sh-Myc, showed complete shutdown of c-Myc expression following the addition of tetracycline (supplementary material Fig. S5A). In a time course study, we found that 1 µg/ml of tetracycline was sufficient to shut down c-Myc expression for up to 24 hours (supplementary material Fig. S5B). Titration with different concentrations of tetracycline revealed that 0.5 µg/ml of the antibiotic led to an almost complete shutdown of c-Myc protein expression within 12 hours (supplementary material Fig. S5C).

Since the ability of the cells to penetrate through a barrier of reconstituted basement membrane correlates with their invasive potential, we carried out *in vitro* matrigel invasion assays with HCT116 sh-Myc and HCT116 BLM^{-/-} sh-Myc cells in (see Material and Methods) presence and absence of tetracycline. Both the partial and total absence of c-Myc (obtained by using two different concentrations of tetracycline) decreased the invasive potential of the cells by almost half (compare the normal BLM⁺ c-Myc⁺ genotype with BLM⁺ c-Myc⁻ conditions under which Myc is decreased to a different extent). This indicates that the percentage of invasive HCT116 cells is largely

due to c-Myc expression (Fig. 7A; supplementary material Fig. S6). However, compared with the normal condition (BLM⁺ c-Myc⁺ genotype), absence of BLM in presence of c-Myc (i.e. BLM⁻ c-Myc⁺ genotype) statistically enhanced invasive capability of the cells ~1.6 times, indicating that BLM is a crucial component regulating the invasive potential of c-Myc (Fig. 7A).

To conclusively link the increased invasive potential of cells that express c-Myc but lack BLM (Fig. 7A) to the action of BLM on Fbw7, *in vitro* matrigel invasion assays were carried out in parallel in HCT116 (wild type) or HCT116 Fbw7^{-/-} cells, in which the expression of BLM was shut down by transfecting its cognate siRNA (Fig. 7B, top). As expected, owing to their respective tumor suppressive functions, ablation of BLM or Fbw7 alone mildly enhanced the invasion potential of the cells (Fig. 7B, bottom). However, lack of both Fbw7 and BLM, i.e. BLM⁻ Fbw7^{-/-} genotype, which should also indicate the BLM⁻ c-Myc⁺ genotype, statistically enhanced the invasive potential five- to sixfold (Fig. 7B, bottom). The invasive potential of BLM⁻ Fbw7^{-/-} cells was higher compared with BLM⁻ c-Myc⁺ cells (compare their respective invasion percentages in Fig. 7A,B). The effect of BLM on the stability of other SCF^{Fbw7} substrates, such as cyclin E and c-Jun, might also contribute during the invasion process.

Next, the above studies were extended to a xenograft model in nude mice. The generated stable cell lines were subcutaneously injected into nude mice. Feeding of tetracycline to 50% of the animals led to the generation of four different genotypes within the microenvironment of the injected cells. The absence of BLM staining in HCT116 BLM^{-/-} derivatives and ablation of c-Myc staining after tetracycline treatment were confirmed in the respective tumor sections (supplementary material Fig. S7). In accordance with the role of BLM as a tumor suppressor, its absence alone mildly accelerated tumor initiation [compare BLM⁺ c-Myc⁺ (9.1 days) with BLM⁻ c-Myc⁺ (5.4 days)]. Lack of c-Myc delayed tumor initiation in presence of BLM [compare BLM⁺ c-Myc⁺ (9.1 days) with BLM⁺ c-Myc⁻ (16.6 days)] and in absence of BLM [compare BLM⁻ c-Myc⁺ (5.4 days) with BLM⁻ c-Myc⁻ (9.2 days)] (Fig. 7C). The delayed initiation of tumor formation owing to BLM expression (~1.7 times) was statistically significant ($P=0.044$). Significantly, the initiation of the tumor formation was most delayed when BLM expression occurred in the absence of c-Myc [compare BLM⁺ c-Myc⁻ (16.6 days) with any other genotype], thereby indicating that – apart from its intrinsic function as a tumor suppressor – BLM can also act on c-Myc, enhance its degradation and, thereby, delay tumor initiation to the maximal extent.

The role of c-Myc in diverse functions led us to determine the levels of proliferation and apoptosis in the tumor sections derived from nude mice through Ki67 staining and TUNEL assay (Fig. 7D; supplementary material Fig. S7). The net proliferative capacity of the tumors (measured as the ratio of proliferation versus apoptosis) was decreased by the loss of c-Myc (compare BLM⁺ c-Myc⁺ with BLM⁺ c-Myc⁻) and increased by the loss of BLM (compare BLM⁻ c-Myc⁺ with BLM⁻ c-Myc⁻). Since the rate of proliferation is lower in BLM⁺ c-Myc⁻, the tumor initiates later in these cells within the mouse xenograft model compared with BLM⁺ c-Myc⁺ (Fig. 7C). Loss of BLM together with the presence of c-Myc increased the net proliferative capacity of the tumors (compare BLM⁻ c-Myc⁺ with any other genotypes). Expression of CD31 (a marker that

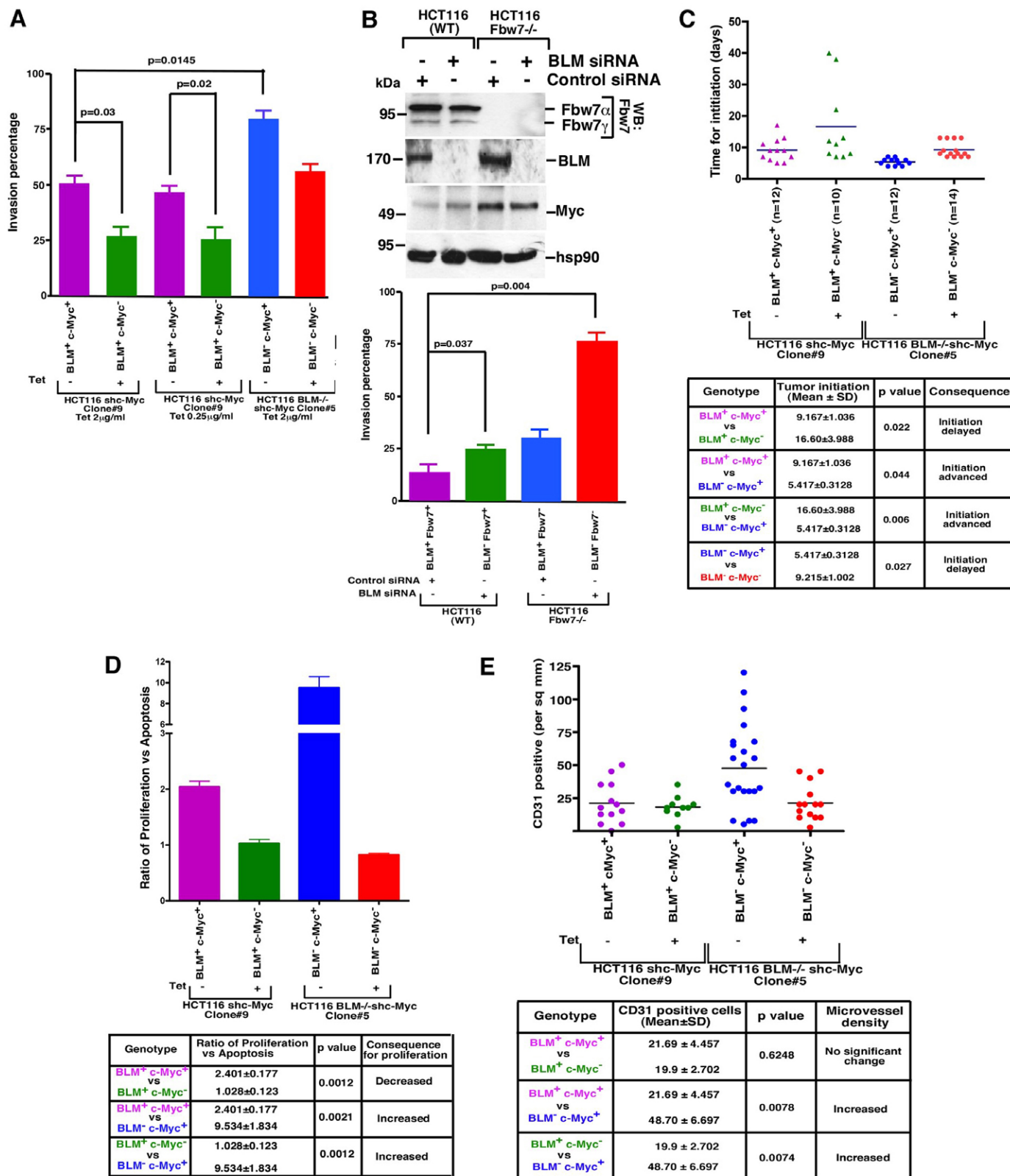


Fig. 7. See next page for legend.

indicates the extent of angiogenesis) was also highest in tumor sections of mice with a $BLM^- c-Myc^+$ genotype (Fig. 7E; supplementary material Fig. S7). Together, these results indicate that the negative regulation of c-Myc stability through BLM lead to a delay in tumor initiation in nude mice (supplementary material Fig. S8).

Discussion

Apart from predisposition to multiple forms of cancer in BS patients (German, 1997), enhanced risk of colorectal cancer is also apparent in individuals who are heterozygous for the BLM^{Ash} alleles (Gruber et al., 2002). Enhanced tumor formation also occurs in mice that are heterozygous for Blm mutation (Goss et al., 2002). These mutant mice develop twice the number of intestinal tumors when crossed with mice that carry a mutation in the Apc tumor suppressor. We now provide mechanistic evidence how BLM may control the early stage of colorectal tumorigenesis. Dissecting the role of BLM in relation to c-Myc during neoplastic transformation was carried out using colon-cancer-derived HCT116 derivatives (Fig. 7). Incidentally, Myc has been identified as a target of the Apc pathway (He et al., 1998). c-Myc is overexpressed at the RNA and protein levels at both early and late stages of almost 70% of colorectal tumors (Finley et al., 1989; Sikora et al., 1987), and in multiple colon carcinoma cell lines, including HCT116 (He et al., 1998). On the basis of the known functions of c-Myc, it is not surprising that the decrease in c-Myc expression lowers the invasive capability of the cells, delays the tumor initiation and decreases the ratio of proliferation versus apoptosis (Fig. 7A,C,D, compare $BLM^+ c-Myc^+$ with $BLM^- c-Myc^-$ in each case). What is more significant is that the loss of BLM increases the invasive potential of the c-Myc-expressing cells, advances the time for tumor initiation in the xenograft model, increases the ratio of proliferation versus apoptosis and increases the expression of the angiogenesis marker, CD31 (Fig. 7A,C,D, compare $BLM^+ c-Myc^+$ with

$BLM^- c-Myc^+$ in each case). In combination with the biochemical data and the evidence obtained using endogenous proteins (Figs 1-5), the effect of BLM on c-Myc target genes (Fig. 6; supplementary material S4E,F; Tables S1, S2), the results from the xenograft mice model (Fig. 7) led us to believe that the delay in tumor initiation is a reflection of the negative regulatory effect of BLM on c-Myc stability and, subsequently, on the subset of c-Myc target genes, whose expression is controlled by the helicase.

Oncogenes such as Ras frequently synergize with Myc during the transformation process (Pelengaris et al., 2002). In the genetic model of colorectal tumorigenesis (Fearon and Vogelstein, 1990), Ras mutations are thought to be the initiating event in a subset of colorectal tumors. Adenomas with Ras mutations are more likely to progress than adenomas without Ras mutations. HCT116 cells also contain an activating Ras mutation. Tumors from HCT116 cells that lack the mutant Ras allele have been shown to be non-tumorigenic (Shirasawa et al., 1993), indicating that Ras is the dominant tumorigenic factor in these cells. Oncogenic Ras in HCT116 carries out its function by upregulating c-Myc levels (Ihle et al., 2009) by affecting the mRNA and the protein stability (Lloyd et al., 1989; Sears et al., 1999). Hence, we hypothesize that BLM – by deregulating c-Myc during tumor initiation – also indirectly affects functions of activated Ras during the initiation step of colorectal tumorigenesis.

A large body of literature exists that has detailed the role of BLM as a helicase (Bachrati and Hickson, 2008). However, evidence has accumulated that conclusively demonstrated the role of BLM as a sensor of DNA lesion, acting in multiple steps of the DNA-damage-response pathway (Tikoo and Sengupta, 2010). It is tempting to speculate that BLM, by acting as a sensor of DNA damage, can also help stalling continuous rounds of cell cycles by negatively regulating Myc expression levels and, thereby, maintaining the genomic stability. Enhancement of c-Myc degradation and, thereby, negative regulation of tumor initiation provides further evidence for the helicase-independent function of BLM. This function of BLM, together with its roles during the multiple steps of the DNA-damage-signaling cascade (Tikoo and Sengupta, 2010), account for the function of BLM as a caretaker tumor suppressor.

It is known that $Fbw7$ binds to c-Myc after the latter is phosphorylated through $GSK3\beta$ within the phospho-degron motif $Cdc4$ phospho-degron (CPD), thereby initiating the degradation of c-Myc (Welcker and Clurman, 2008). However, parallel mechanisms of c-Myc ubiquitylation and degradation also exist. $Skp2$, another E3 ligase, is known to mediate phosphorylation independent degradation of c-Myc as well as its transcriptional activation (Kim et al., 2003; von der Lehr et al., 2003). We have provided evidence that the effect of BLM is specifically on $Fbw7$ and not $Skp2$ (Fig. 3D). Furthermore, we have demonstrated that the BLM-mediated enhancement in the c-Myc- $Fbw7$ interaction is not dependent on a specific phosphorylation of c-Myc at Thr58 and Ser62 (supplementary material Fig. S3B,E). However, phosphorylation within the CPD is an essential requirement for BLM to subsequently enhance c-Myc ubiquitylation and, thereby, causing its degradation (Fig. 5C; supplementary material S4B-D). These results indicate that the effect of BLM in enhancing c-Myc ubiquitylation through degradation acts in conjunction with its known principal mechanism of turnover. Apart from $GSK3\beta$, other kinases such as $Pim1$ and $Pim2$ are also known to be involved in the degradation of c-Myc (Zhang et al., 2008).

Fig. 7. c-Myc dependent tumor initiation is regulated by BLM. (A) Loss of BLM enhances c-Myc invasiveness. Graphical representation of the invasion percentage of HCT116 $BLM^{-/-}$ sh-Myc Clone#5 and HCT116 sh-Myc Clone#9 grown in absence or presence of different concentrations of tetracycline. (B) Loss of both BLM and $Fbw7$ enhances the invasiveness of HCT116 cells. (Top) HCT116 (WT) or HCT $Fbw7^{-/-}$ cells have been transiently transfected with either BLM siRNA or Control siRNA. Post-transfection the whole cell lysates are made and ran on SDS-PAGE gels and probed with antibodies against $Fbw7$, BLM (A300-110A), c-Myc (#9402) and $hsp90$. (Bottom) Graphical representation of the invasion percentage of HCT116 (WT) or HCT116 $Fbw7^{-/-}$ cells transfected with either Control siRNA or BLM siRNA. (C) Initiation of tumor is advanced due to loss of BLM in a c-Myc-dependent manner in mouse xenograft model. Graphical representation of tumor initiation after HCT116 $BLM^{-/-}$ sh-Myc Clone#5 and HCT116 sh-Myc Clone#9 clones have been subcutaneously injected into nude mice. Half of the mice injected with each cell type are fed with tetracycline and tumor initiation monitored for all mice. Comparison for the mean day of tumor initiation is represented. The total number of mice in each group is denoted by n. (D) Ratio of proliferation versus apoptosis in tumor sections is enhanced due to loss of BLM in a c-Myc-dependent manner. Same as C, except that tumors obtained from all mice at 18 days post-injection are used. Graphical representation of the ratio of proliferation (stained with Ki67) versus apoptosis (determined by TUNEL) observed in tumor sections for different genotypes is represented. (E) CD31 positive cells in tumor sections are enhanced due to loss of BLM in a c-Myc-dependent manner. Same as D, except that graphical representation of the extent of CD31-positive cells observed in tumor sections for different genotypes are represented.

Indeed, *Pim1* is one of the c-Myc target genes that is also regulated by BLM (supplementary material Tables S1 and S2), and is highly expressed in cells that express BLM at both the RNA and protein level (see *Pim1* transcript and protein levels in Fig. 6C-E). Overall, the enhancement of Fbw7, mediated c-Myc degradation through BLM falls under an expanding category of additional regulatory circuitry that mediates c-Myc turnover.

Owing to its expression profile in diverse forms of cancer, c-Myc and c-Myc-driven pathways remain very attractive targets for anti-cancer therapy (Soucek et al., 2008). A variety of strategies have been suggested (Albihn et al., 2010), some of which are in the pre-clinical stage. It is interesting to note that, despite being an attractive target, till now not a single c-Myc-specific therapy is presently approved for clinical trials (<http://clinicaltrials.gov/>). A therapy, on the basis of a decreased half-life of c-Myc, that uses derivatives of BLM could be an attractive option. Oncogene-induced replicative stress has already been shown to be effective in killing c-Myc-driven tumors (Murga et al., 2011). Efforts maybe directed to obtain BLM derivatives that can increase c-Myc ubiquitylation and, hence, enhance its degradation.

Materials and Methods

Recombinants and siRNA

pGEX4T-1 BLM (1-1417) (Srivastava et al., 2009), pGEX4T-1 BLM (1-212), pcDNA3 Flag BLM (gift from Ian Hickson), EGFP-C1 BLM (gift from Nathan Ellis), pGEX4T-1 BLM (191-660), pGEX4T-1 BLM (621-1041), pGEX4T-1 BLM (1001-1417) (Tripathi et al., 2008), pSG5-Jun (gift from Bohdan Wasyluk), pcDNA3 Cyclin E (Origene), pcDNA3 c-Myc (gift from Eric Huang and Izumi Horikawa), pGEX4T-1 c-Jun (1-331), pGEX4T-1 c-Jun (1-313), pGEX4T-1 c-Jun (1-241), pGEX4T-1 c-Myc (1-439), pGEX4T-1 c-Myc (1-203), pGEX4T-1 c-Myc (1-237), pGEX4T-1 c-Myc (238-439), pGEX4T-1 c-Myc (238-410), pGEX4T-1 c-Myc (238-368), pGEX4T-1 c-Myc (238-300), pGEX4T-1 c-Myc (300-439), pGEX4T-1 c-Myc (368-439), pGEX4T-1 c-Myc (410-439) and pGEX4T-1 c-Myc (300-410) were obtained by cloning the respective PCR products into the EcoRI/XhoI sites of the vector. pGEX4T-1 c-Myc (Δ 300-410) was generated by a two-step cloning process. In the first step pGEX4T-1 c-Myc (1-299) was generated by cloning the PCR fragment into the *Bam*H1-*Eco*R1 site of pGEX4T-1. In the second step c-Myc (411-439) was inserted in frame with c-Myc (1-299) at *Eco*R1-*Xho*I sites to generate pGEX4T-1 c-Myc (Δ 300-410). pMAL Myc (1-451) was obtained by cloning the PCR fragment into the *Eco*R1-*Hind*III sites of pMAL-p2X vector. 3pX-Flag-myc-CMV-24 Fbw7 α , 3pX-Flag-myc-CMV-24 Fbw7 β , 3pX-Flag-myc-CMV-24 Fbw7 γ , 3pX-Flag-myc-CMV-24 Fbw7 δ , 3pX-Flag-myc-CMV-24 Fbw7 ϵ , 3pX-Flag-myc-CMV-24 Fbw7 ζ , 3pX-Flag-myc-CMV-24 Fbw7 η and 3pX-Flag-myc-CMV-24 Fbw7 θ (which contains only the common region of the three Fbw7 isoforms) and pFLAG-Fbw7 Δ (gift from Markus Welcker and Bruce Clurman), pET28b-Fbw7 γ was obtained by cloning the PCR fragment into the *Eco*R1/*Not*I sites of pET28b vector. pcDNA6TR (Invitrogen), pTER-c-Myc (gift from Marc van de Wetering), siRNA for Fbw7 (On target plus Smart Pool) was purchased from Dharamacon. siRNA for BLM (custom synthesis against the sequence 5'-AGCAGCGAUGUGAUUUGCA-3') was purchased from Dharamacon. ON-TARGET plus non-targeting siRNA #1 from Dharamacon (D-001810-01-05) was used as the control siRNA. All transfections were carried out using Lipofectamine 2000 (Invitrogen). All siRNA transfections were carried out for 54 hours.

Antibodies

Anti-BLM: ab476 (Abcam), A300-110A (Bethyl), A300-120A (Bethyl), HPA005689 (Sigma). Anti-c-Myc: 13-2500, Clone 9E10 (Invitrogen), #9402 (Cell Signaling), sc-764, N-262 (Santa Cruz Biotechnology), ab39688 (Abcam). Anti-phosphorylated c-Myc (Thr58/Ser62): sc-8000-R (Santa Cruz Biotechnology). Anti-WRN: NB100-140 (Novus Biologicals). Anti-RECQL4: K6312 (De et al., 2012). Anti-Cyclin E: 551159 (BD Pharmingen). Anti-c-Jun: ab31419 (Abcam). Anti-B MyB: ab12296 (Abcam). Anti-KLF5: ab24331 (Abcam). Anti-Actin: sc-8432 (Santa Cruz Biotechnology). Anti-Flag: F1804 (Sigma). Anti-Flag antibody beads: A2220 (Sigma). Anti-Fbw7: ab74054 Clone 3a9/1 (Abcam). Anti-polyHistidine: H1029 (Sigma). Anti-mono and poly ubiquitylated conjugates (Clone FK2): PW8810 (Enzo Life Sciences). Anti-K48 polyubiquitin: Apu2.07 (gift from Vishva M. Dixit). Anti-NPM1: ab15440 (Abcam). Anti-RPL27: ab74731 (Abcam). Anti-MIF: ab7207 (Abcam). Anti-MITF: ab12039 (Abcam). Anti-EGFR: ab2430. Anti-PIM1: ab66767 (Abcam). Anti-p53R2: ab8105 (Abcam). Anti-CDH2: ab19348 (Abcam). Anti-hsp90: sc-7947 (Santa Cruz Biotechnology). Anti-GSK3 β (phospho S9) antibody: ab9769 (Abcam). Anti-CD31: ab28364 (Abcam). Anti-Ki67: ab166667 (Abcam).

Cell culture conditions, treatments and assays

hTERT-immortalized Bloom Syndrome fibroblasts from a Bloom Syndrome patient GM03509 (referred as BS cells) and chromosome 15 mini-chromosome-corrected BS fibroblasts GM03509 (referred as A-15 cells) were maintained as described (Sengupta et al., 2003). Fibroblasts from another BS patient GM08505 were immortalized and complemented either with GFP + BLM (referred as GM08505 + GFP-BLM cells) or with GFP alone (referred as GM08505 + GFP) (gift from Nathan Ellis) (Hu et al., 2001). The colorectal carcinoma cell line HCT116 and its isogenic counterpart in which BLM has been deleted through homologous recombination are referred to as HCT116 BLM^{-/-} (gift from Bert Vogelstein) (Rajagopalan et al., 2004). HCT116 and HCT116 Fbw7^{-/-} (gift from Jonathan Grim and Bruce Clurman) (Grim et al., 2008). 73-26hTERT and 73-26hTERT-WRN (gift from Judith Campisi) (Yannone et al., 2001). AG05139, AG03587, D8903644-K and B1865425K (De et al., 2012). LLnL (25 μ M, Sigma) or MG132 (25 μ M, Calbiochem) treatments were carried out for the final 3 h of the incubation. Cycloheximide (1 mM, Sigma) was added for either 2 hours or 6 hours, in cells grown in presence of serum. For pulse-chase experiments, cells were treated with 700 μ Ci S³⁵-methionine (Board of Radiation and Isotope Technology, India) in serum-free, methionine-free medium for 30 minutes. The cells were subsequently washed and were grown for the indicated times in normal medium. The concentrations and amounts used for different treatments were: GSK3 β inhibitor VIII (Calbiochem): 25 μ M, λ phosphatase (New England Biolabs): 100 units. GSK3 β inhibitor VIII and λ phosphatase were incubated with c-Myc for 1 hour prior to the interaction or ubiquitylation at 30°C or 37°C, respectively. GSK3 β activity was measured using an assay kit (CS0990, Sigma) with γ -³²P-ATP according to the manufacturer's protocol.

In vitro ubiquitylation

SCF^{Fbw7 α} and SCF^{Fbw7 γ} were obtained by transfecting 3pX-Flag-myc-CMV-24 Fbw7 α , 3pX-Flag-myc-CMV-24 Fbw7 γ or pFLAG-Fbw7 Δ F into 293T cells. The SCF^{Fbw7} E3 complexes or its non-functional Fbw7 Δ F mutant were purified from the cells by immunoprecipitation (IP) using anti-Flag antibody beads, eluted out using Flag peptide (Sigma), checked for purity, evaluated and used for ubiquitylation assays. For ubiquitylation assays, 1 μ l of *in vitro* translated c-Myc (~30 ng of the protein) was incubated at 30°C for 1 hour with 100 ng of Uba1 (Calbiochem), 200 ng of UbcH5a (Calbiochem) and 6 μ g of purified ubiquitin (Boston Biochem) and 0.5-2 μ l of the eluted E3 ligase (depending on its activity). The reaction was carried out in a final volume of 20 μ l in a ubiquitylation buffer containing 4 mM HEPES-NaOH (pH 7.9), 6 mM potassium acetate, 0.2 mM DTT, 0.5 mM MgCl₂, 0.05 mM EDTA, 1% glycerol and 0.15 mM ATP. Soluble GST-tagged BLM (wild type or its derivatives), GSK3 β inhibitor or λ phosphatase were included as indicated.

Northern analysis, reverse-transcriptase PCR, real-time PCR

Total RNA was isolated by Trizol reagent (Invitrogen). Northern analysis was done using 20 μ g of the total RNA using the entire c-Myc (1-439) open reading frame as the probe. For reverse-transcriptase (RT)-PCR the primers used are listed in supplementary material Table S3. Taqman gene expression assays for *Myc* and *Actb* (β actin) were obtained from Applied Biosystems. Real-time PCR analysis for the c-Myc target genes that were also regulated by BLM was carried out using customized TaqMan array 96-well plates (Catalog number 4413256). All RT-PCR and real-time PCR analyses were done at least thrice (each time in duplicates) in ABI PRISM 7000 according to manufacturer's instructions (Invitrogen).

Transfections, immunofluorescence, microscope image acquisition

Transfection for immunofluorescence experiments was carried out on coverslips by using Lipofectamine 2000 (Invitrogen) according to manufacturer's protocol. Cytoplasmic and nuclear extracts from cells were made using NE-PER Nuclear and Cytoplasmic Extraction Reagent (Pierce). For preparation of whole-cell lysates, the cells were lysed in RIPA buffer. For immunofluorescence, the cells were washed and fixed with ice-cold methanol:acetone (1:1) for 5 minutes before immunostaining. For confocal microscopy, the slides were analyzed on a Zeiss 510 Meta system with 63 \times /1.4 oil immersion objective. The laser lines used were Argon 458/477/488/514 nm (for EGFP), DPSS 561 nm (for Texas Red) and a Chameleon Ultra autotunable femtosecond laser with a tuning range of 690-1050 nm (for DAPI). LSM5 software was used for image acquisition. Quantification was carried out after visualization of 200 cells. Numbers indicate the percentage of cells that show colocalization of the two proteins.

Microarray hybridization

Total RNA obtained from BS and A-15 cells was used for microarray gene expression analysis. The Applied Biosystems human genome survey microarray version 2.0 chip containing 32,878 oligonucleotide probes (60-mer) representing 29,098 individual human genes and more than 1000 control probes was used for microarray profiling. Digoxigenin-UTP-labeled cRNA was generated and linearly amplified from 1 μ g of total RNA from each sample by using an Applied Biosystems Chemiluminescent reverse-transcription *in-vitro* transcription

(RT-IVT) labeling kit according to the manufacturer's protocol. Duplicate microarray hybridizations were carried out and the raw data values of intensities were normalized using trimmed mean scale. Chemiluminescence detection and image acquisition were performed according to the manufacturer's protocol (Applied Biosystems). Signals were quantified and corrected for background, and final images and feature data were processed by using Applied Biosystems 1700 Chemiluminescent Microarray Analyzer software version 1.1. Obtained were lists of genes that were differentially expressed in the absence of BLM (>twofold change at 95% confidence with signal-to-noise ratio ≥ 3).

Generation of inducible stable lines

Stable cell lines HCT116 sh-Myc and HCT116 BLM^{-/-} sh-Myc were generated using the tetracycline repressor, pcDNA6TR (Invitrogen) and a short hairpin RNA against *Myc* cloned into pTER vector, pTER *c-myc* (van de Wetering et al., 2003). The two plasmids were co-transfected into HCT116 BLM^{+/+} and HCT116 BLM^{-/-} cell lines at the ratio 10 μ g:1 μ g (pcDNA6TR:pTER *c-myc*) using Lipofectamine 2000 (Invitrogen). After phenotypic expression the cells were grown for 4 days in selective medium containing 15 μ g/ml of blasticidin (Invitrogen) and 450 μ g/ml zeocin (Invitrogen) to obtain the respective clones.

Matrigel-invasion assays

Matrigel-invasion assays were carried out in 6-well BD Biocoat Matrigel Invasion Chambers (BD Biosciences) according to the manufacturer's protocol. Tetracycline-inducible cell lines were grown in serum-free medium (in absence or presence of tetracycline) for 12 hours before being used for the assay. Post-invasion, the membranes were removed and observed at 40 \times magnification after staining with 1% Toluidine Blue (Fluka) in 1% borax (Sigma) for 2 minutes. The entire experiment was repeated in parallel with control inserts. Percentage invasion was determined by the relative ratio of the mean number of cells invading through the matrigel insert membrane versus the number of cells invading through the control-insert membrane. The invasion assays were also carried out in parallel using HCT116 and HCT116 Fbw7^{-/-} cells after transfecting them with siRNA BLM or siRNA control. Post-transfection the cells were either lysed to be checked for western analysis or trypsinized for setting up the invasion assays. All experiments were set up at least in triplicates and repeated independently three times. The *P*-values were obtained by using two-tailed student's *t*-test, unpaired data with unequal variance. Values are mean \pm s.d.

Nude mice experiments

6 \times 10⁶ cells in 100 μ l medium were mixed with matrigel (1:1 ratio) and injected subcutaneously into 6-weeks old female nude mice. For the entire duration of the experiment 50% of the mice were made to drink 5% sucrose water, whereas the rest drank 0.5 μ g/ml tetracycline in 5% sucrose water. Mice were observed every day for tumor initiation (i.e. detecting tumors of at least 2–3 mm³). The tumors were manually measured with calipers and the size was estimated using the ellipsoid formula of height \times width \times length \times 0.5 (mm³). All work on nude mice has been carried out in accordance with and approval of the National Institute of Immunology Animal Ethics Committee.

Acknowledgements

The authors like to acknowledge Ian Hickson, Nathan Ellis, Eric Huang, Izumi Horikawa, Markus Welcker, Bruce Clurman, Marc van de Wetering and Bohdan Wasyluk for plasmids, Vishva M. Dixit for antibodies, Nathan Ellis, Bert Vogelstein, Judith Campisi, Bruce Clurman and Jonathan Grim for cells. The authors declare that they do not have any conflicting commercial interest regarding the work described in the manuscript.

Author contributions

S.C., R.P., V.M., S.T., M.H., R.M., P.M. and V.S. carried out the experiments. S.S. analyzed the data and wrote the manuscript.

Funding

The authors acknowledge National Institute of Immunology core funds, Department of Biotechnology (DBT), India (BT/PR11258/BRB/10/645/2008), Department of Science and Technology (DST), India (SR/SO/BB-08/2010), Indo-French Centre for the Promotion of Advanced Research (IFPAR) (IFC/4603-A/2011/1250) and Council of Scientific and Industrial Research (CSIR), India [37(1541)/12/EMR-II] for financial assistance.

Supplementary material available online at

<http://jcs.biologists.org/lookup/suppl/doi:10.1242/jcs.124719/-DC1>

References

- Albihn, A., Johnsen, J. I. and Henriksson, M. A. (2010). MYC in oncogenesis and as a target for cancer therapies. *Adv. Cancer Res.* **107**, 163–224.
- Arabi, A., Wu, S., Ridderstråle, K., Bierhoff, H., Shiu, C., Fatyol, K., Fahlén, S., Hydbring, P., Söderberg, O., Grummt, I. et al. (2005). c-Myc associates with ribosomal DNA and activates RNA polymerase I transcription. *Nat. Cell Biol.* **7**, 303–310.
- Bachrati, C. Z. and Hickson, I. D. (2008). RecQ helicases: guardian angels of the DNA replication fork. *Chromosoma* **117**, 219–233.
- Bugreev, D. V., Yu, X., Egelman, E. H. and Mazin, A. V. (2007). Novel pro- and anti-recombination activities of the Bloom's syndrome helicase. *Genes Dev.* **21**, 3085–3094.
- Chaganti, R. S., Schonberg, S. and German, J. (1974). A manyfold increase in sister chromatid exchanges in Bloom's syndrome lymphocytes. *Proc. Natl. Acad. Sci. USA* **71**, 4508–4512.
- Dai, M. S., Jin, Y., Gallegos, J. R. and Lu, H. (2006). Balance of Yin and Yang: ubiquitylation-mediated regulation of p53 and c-Myc. *Neoplasia* **8**, 630–644.
- Dang, C. V., O'Donnell, K. A., Zeller, K. I., Nguyen, T., Osthus, R. C. and Li, F. (2006). The c-Myc target gene network. *Semin. Cancer Biol.* **16**, 253–264.
- De, S., Kumari, J., Mudgal, R., Modi, P., Gupta, S., Futami, K., Goto, H., Lindor, N. M., Furuichi, Y., Mohanty, D. et al. (2012). RECQL4 is essential for the transport of p53 to mitochondria in normal human cells in the absence of exogenous stress. *J. Cell Sci.* **125**, 2509–2522.
- Fearon, E. R. and Vogelstein, B. (1990). A genetic model for colorectal tumorigenesis. *Cell* **61**, 759–767.
- Finley, G. G., Schulz, N. T., Hill, S. A., Geiser, J. R., Pipas, J. M. and Meisler, A. I. (1989). Expression of the myc gene family in different stages of human colorectal cancer. *Oncogene* **4**, 963–971.
- German, J. (1997). Bloom's syndrome. XX. The first 100 cancers. *Cancer Genet. Cytogenet.* **93**, 100–106.
- Goss, K. H., Risinger, M. A., Kordich, J. J., Sanz, M. M., Straughen, J. E., Slovek, L. E., Capobianco, A. J., German, J., Boivin, G. P. and Groden, J. (2002). Enhanced tumor formation in mice heterozygous for BLM mutation. *Science* **297**, 2051–2053.
- Grim, J. E., Gustafson, M. P., Hirata, R. K., Hagar, A. C., Swanger, J. E., Welcker, M., Hwang, H. C., Ericsson, J., Russell, D. W. and Clurman, B. E. (2008). Isoform- and cell cycle-dependent substrate degradation by the Fbw7 ubiquitin ligase. *J. Cell Biol.* **181**, 913–920.
- Gruber, S. B., Ellis, N. A., Scott, K. K., Almog, R., Kolachana, P., Bonner, J. D., Kirchhoff, T., Tomsho, L. P., Nafa, K., Pierce, H. et al. (2002). BLM heterozygosity and the risk of colorectal cancer. *Science* **297**, 2013.
- Hann, S. R. (2006). Role of post-translational modifications in regulating c-Myc proteolysis, transcriptional activity and biological function. *Semin. Cancer Biol.* **16**, 288–302.
- He, T. C., Sparks, A. B., Rago, C., Hermeking, H., Zawel, L., da Costa, L. T., Morin, P. J., Vogelstein, B. and Kinzler, K. W. (1998). Identification of c-MYC as a target of the APC pathway. *Science* **281**, 1509–1512.
- Hickson, I. D. (2003). RecQ helicases: caretakers of the genome. *Nat. Rev. Cancer* **3**, 169–178.
- Hu, P., Beresten, S. F., van Brabant, A. J., Ye, T. Z., Pandolfi, P. P., Johnson, F. B., Guarente, L. and Ellis, N. A. (2001). Evidence for BLM and Topoisomerase IIIalpha interaction in genomic stability. *Hum. Mol. Genet.* **10**, 1287–1298.
- Ihle, N. T., Lemos, R., Jr, Wipf, P., Yacoub, A., Mitchell, C., Siwak, D., Mills, G. B., Dent, P., Kirkpatrick, D. L. and Powis, G. (2009). Mutations in the phosphatidylinositol-3-kinase pathway predict for antitumor activity of the inhibitor PX-866 whereas oncogenic Ras is a dominant predictor for resistance. *Cancer Res.* **69**, 143–150.
- Kim, S. Y., Herbst, A., Tworowski, K. A., Salghetti, S. E. and Tansey, W. P. (2003). Skp2 regulates Myc protein stability and activity. *Mol. Cell* **11**, 1177–1188.
- Lloyd, A. C., Paterson, H. F., Morris, J. D., Hall, A. and Marshall, C. J. (1989). p21H-ras-induced morphological transformation and increases in c-myc expression are independent of functional protein kinase C. *EMBO J.* **8**, 1099–1104.
- Murga, M., Campaner, S., Lopez-Contreras, A. J., Toledo, L. I., Soria, R., Montaña, M. F., D'Artista, L., Schleker, T., Guerra, C., Garcia, E. et al. (2011). Exploiting oncogene-induced replicative stress for the selective killing of Myc-driven tumors. *Nat. Struct. Mol. Biol.* **18**, 1331–1335.
- Nesbit, C. E., Tersak, J. M. and Prochowik, E. V. (1999). MYC oncogenes and human neoplastic disease. *Oncogene* **18**, 3004–3016.
- Pelengaris, S., Khan, M. and Evan, G. (2002). c-MYC: more than just a matter of life and death. *Nat. Rev. Cancer* **2**, 764–776.
- Rajagopalan, H., Jallepalli, P. V., Rago, C., Velculescu, V. E., Kinzler, K. W., Vogelstein, B. and Lengauer, C. (2004). Inactivation of hCDC4 can cause chromosomal instability. *Nature* **428**, 77–81.
- Russell, B., Bhattacharyya, S., Keirse, J., Sandy, A., Grierson, P., Perchiniak, E., Kavcansky, J., Acharya, S. and Groden, J. (2011). Chromosome breakage is regulated by the interaction of the BLM helicase and topoisomerase IIIalpha. *Cancer Res.* **71**, 561–571.
- Sears, R., Leone, G., DeGregori, J. and Nevins, J. R. (1999). Ras enhances Myc protein stability. *Mol. Cell* **3**, 169–179.
- Sengupta, S., Linke, S. P., Pedoux, R., Yang, Q., Farnsworth, J., Garfield, S. H., Valerie, K., Shay, J. W., Ellis, N. A., Wasyluk, B. et al. (2003). BLM helicase-dependent transport of p53 to sites of stalled DNA replication forks modulates homologous recombination. *EMBO J.* **22**, 1210–1222.

- Shirasawa, S., Furuse, M., Yokoyama, N. and Sasazuki, T.** (1993). Altered growth of human colon cancer cell lines disrupted at activated Ki-ras. *Science* **260**, 85-88.
- Sikora, K., Chan, S., Evan, G., Gabra, H., Markham, N., Stewart, J. and Watson, J.** (1987). c-myc oncogene expression in colorectal cancer. *Cancer* **59**, 1289-1295.
- Soucek, L., Whitfield, J., Martins, C. P., Finch, A. J., Murphy, D. J., Sodik, N. M., Karnezis, A. N., Swigart, L. B., Nasi, S. and Evan, G. I.** (2008). Modelling Myc inhibition as a cancer therapy. *Nature* **455**, 679-683.
- Srivastava, V., Modi, P., Tripathi, V., Mudgal, R., De, S. and Sengupta, S.** (2009). BLM helicase stimulates the ATPase and chromatin-remodeling activities of RAD54. *J. Cell Sci.* **122**, 3093-3103.
- Sullivan, N. F., Willis, A. E., Moore, J. P. and Lindahl, T.** (1989). High levels of the c-myc protein in cell lines of Bloom's syndrome origin. *Oncogene* **4**, 1509-1511.
- Tikoo, S. and Sengupta, S.** (2010). Time to bloom. *Genome Integr.* **1**, 14.
- Tikoo, S., Madhavan, V., Hussain, M., Miller, E. S., Arora, P., Zlatanou, A., Modi, P., Townsend, K., Stewart, G. S. and Sengupta, S.** (2013). Ubiquitin-dependent recruitment of the Bloom Syndrome helicase upon replication stress is required to suppress homologous recombination. *EMBO J.* **32**, 1778-1792.
- Tripathi, V., Nagarjuna, T. and Sengupta, S.** (2007). BLM helicase-dependent and -independent roles of 53BP1 during replication stress-mediated homologous recombination. *J. Cell Biol.* **178**, 9-14.
- Tripathi, V., Kaur, S. and Sengupta, S.** (2008). Phosphorylation-dependent interactions of BLM and 53BP1 are required for their anti-recombinogenic roles during homologous recombination. *Carcinogenesis* **29**, 52-61.
- van de Wetering, M., Oving, I., Muncan, V., Pon Fong, M. T., Brantjes, H., van Leenen, D., Holstege, F. C., Brummelkamp, T. R., Agami, R. and Clevers, H.** (2003). Specific inhibition of gene expression using a stably integrated, inducible small-interfering-RNA vector. *EMBO Rep.* **4**, 609-615.
- von der Lehr, N., Johansson, S., Wu, S., Bahram, F., Castell, A., Cetinkaya, C., Hydbring, P., Weidung, I., Nakayama, K., Nakayama, K. I. et al.** (2003). The F-box protein Skp2 participates in c-Myc proteasomal degradation and acts as a cofactor for c-Myc-regulated transcription. *Mol. Cell* **11**, 1189-1200.
- Welcker, M. and Clurman, B. E.** (2008). FBW7 ubiquitin ligase: a tumour suppressor at the crossroads of cell division, growth and differentiation. *Nat. Rev. Cancer* **8**, 83-93.
- Welcker, M., Orian, A., Grim, J. E., Eisenman, R. N. and Clurman, B. E.** (2004a). A nucleolar isoform of the Fbw7 ubiquitin ligase regulates c-Myc and cell size. *Curr. Biol.* **14**, 1852-1857.
- Welcker, M., Orian, A., Jin, J., Grim, J. E., Harper, J. W., Eisenman, R. N. and Clurman, B. E.** (2004b). The Fbw7 tumor suppressor regulates glycogen synthase kinase 3 phosphorylation-dependent c-Myc protein degradation. *Proc. Natl. Acad. Sci. USA* **101**, 9085-9090.
- West, M. J., Sullivan, N. F. and Willis, A. E.** (1995). Translational upregulation of the c-myc oncogene in Bloom's syndrome cell lines. *Oncogene* **11**, 2515-2524.
- Yada, M., Hatakeyama, S., Kamura, T., Nishiyama, M., Tsunematsu, R., Imaki, H., Ishida, N., Okumura, F., Nakayama, K. and Nakayama, K. I.** (2004). Phosphorylation-dependent degradation of c-Myc is mediated by the F-box protein Fbw7. *EMBO J.* **23**, 2116-2125.
- Yankiwski, V., Marciniak, R. A., Guarente, L. and Neff, N. F.** (2000). Nuclear structure in normal and Bloom syndrome cells. *Proc. Natl. Acad. Sci. USA* **97**, 5214-5219.
- Yannone, S. M., Roy, S., Chan, D. W., Murphy, M. B., Huang, S., Campisi, J. and Chen, D. J.** (2001). Werner syndrome protein is regulated and phosphorylated by DNA-dependent protein kinase. *J. Biol. Chem.* **276**, 38242-38248.
- Yeh, E., Cunningham, M., Arnold, H., Chasse, D., Monteith, T., Ivaldi, G., Hahn, W. C., Stukenberg, P. T., Shenolikar, S., Uchida, T. et al.** (2004). A signalling pathway controlling c-Myc degradation that impacts oncogenic transformation of human cells. *Nat. Cell Biol.* **6**, 308-318.
- Zeller, K. I., Jegga, A. G., Aronow, B. J., O'Donnell, K. A. and Dang, C. V.** (2003). An integrated database of genes responsive to the Myc oncogenic transcription factor: identification of direct genomic targets. *Genome Biol.* **4**, R69.
- Zhang, Y., Wang, Z., Li, X. and Magnuson, N. S.** (2008). Pim kinase-dependent inhibition of c-Myc degradation. *Oncogene* **27**, 4809-4819.